Impact of soil hydraulic parameter uncertainty on soil moisture modeling

Lien Loosvelt,[1] Valentijn R. N. Pauwels,[1] Wim M. Cornelis,[2] Gabriëlle J. M. De Lannoy,[1] and Niko E. C. Verhoest[1]

Received 17 February 2010; revised 30 November 2010; accepted 29 December 2010; published 2 March 2011.

[1] For simulations in basins where soil information is limited to soil type maps, a methodology is presented to quantify the uncertainty of soil hydraulic parameters arising from within-soil-class variability and to assess the impact of this uncertainty on soil moisture modeling. Continuous pedotransfer functions were applied to samples with different texture within each soil class to construct discrete probability distributions of the soil hydraulic parameters. When propagating the parameter distributions through a hydrologic model, a wide range of simulated soil moisture was generated within a single soil class. The pedotransfer function was found to play a crucial role in assessing the uncertainty in the modeled soil moisture, and the geographic origin of the pedotransfer function (region specific versus nonregion specific) highly affected the range and shape of the probability distribution of the soil hydraulic parameters. Furthermore, the modeled soil moisture distribution was found to be non-Gaussian. An accurate uncertainty assessment therefore requires the characterization of its higher-order moments. As an extension of this research, we have shown that applying continuous region-specific pedotransfer functions to the central point of a soil class is a better alternative to standard (often nonregion-specific) class pedotransfer functions for determining an average set of soil hydraulic parameters.

Citation: Loosvelt, L., V. R. N. Pauwels, W. M. Cornelis, G. J. M. De Lannoy, and N. E. C. Verhoest (2011), Impact of soil hydraulic parameter uncertainty on soil moisture modeling, *Water Resour. Res., 47*, W03505, doi:10.1029/2010WR009204.

1. Introduction

[2] Physically based, spatially distributed hydrologic models are important tools for decision making and water management. Unfortunately, these models require large quantities of input data and parameters, which are subject to uncertainty because of imperfect knowledge (epistemic uncertainty) or because of inherent variability (variability uncertainty) [*Walker et al.*, 2003]. Soil hydraulic parameters (SHPs) play a crucial role in hydrologic models as they directly control the movement of water and water balance partitioning. Furthermore, SHPs indirectly control the components of energy balance through the available soil moisture.

[3] There are several ways to determine soil hydraulic parameters, which can be classified into direct and indirect methods. The direct determination of SHPs results from laboratory and field measurements. Among the indirect methods are (1) soil-class pedotransfer functions (PTFs) [e.g., *Rawls et al.*, 1982; *Cosby et al.*, 1984; *Wösten et al.*, 1999], (2) continuous PTFs [e.g., *Vereecken et al.*, 1989; *Rawls and Brakensiek*, 1985; *Schaap et al.*, 1998], and (3) inverse methods [e.g., *Hopmans et al.*, 2002; *Pauwels et al.*, 2009]. Each method comes with certain problems and uncertainties for the modeler. In theory, direct measurement of soil properties provides the best approximation of the true parameters, but at regional scale this procedure is not feasible because of its time consuming and costly nature. Furthermore, the scale at which SHPs are measured is generally incompatible with the scale at which the hydrologic model is applied [e.g., *Grayson et al.*,1992]. As a consequence, good estimates instead of direct measurements may be used for many applications. Therefore, researchers have often relied on relationships between SHPs and soil texture by using PTFs, which translate soil-related information into the hydrologic parameters needed [*Bouma*, 1989]. Since such relations are derived from experimental data under specific conditions, they do not take into account the underlying physical relation, and care should be taken when extrapolating these relations to other regions or ranges of data sets [*Cornelis et al.*, 2001].

[4] Soil-class PTFs link the soil class or measured soil texture to a representative set of parameter values. However, one should be aware that soil classes themselves may not represent the best possible way of classifying soils from a hydraulic point of view, as demonstrated by *Twarakavi et al.* [2010]. Irrespective of the classification system used, uncertain parameters are always obtained because of measurement error, imperfections in the predictive function, or variability in texture. The substantial impact of textural variability on the estimation of various soil hydraulic parameters has been shown in the past [e.g., *Twarakavi et al.*, 2009] and is therefore important to take into account in

[1]Laboratory of Hydrology and Water Management, Ghent University, Ghent, Belgium
[2]Department of Soil Management and Soil Care, Ghent University, Ghent, Belgium

0043-1397/11/2010WR009204

hydrologic studies, since ignoring this uncertainty may compromise hydrologic modeling by not consistently representing system behavior. Earlier research has studied textural variability within soil classes [e.g., *Gutmann and Small*, 2005; *Webb and Lilburne*, 2005; *Vachaud and Chen*, 2002; *Bormann*, 2008] and measurement uncertainty [e.g., *Tietje and Hennings*, 1996; *Finke et al.*, 1996] related to hydrologic modeling.

[5] In practice, simulations are often performed in basins where soil information is limited to soil type maps and knowledge of the exact textural composition is lacking. This forces modelers to rely on class PTFs for estimating SHPs. Unfortunately, this approach creates the following problems with respect to the simulation results: (1) the uncertainty in SHPs because of within-soil-class variability is not incorporated, and (2) nonregion-specific PTFs may be used, resulting in unreliable SHPs. In this paper, both issues are evaluated with respect to modeled uncertainty. The main objectives are to assess uncertainty in the SHPs for simulations in basins with unknown textural composition and to investigate the impact of SHP uncertainty on model prediction uncertainties. An additional objective is to investigate whether the central point of a soil class can be used to generate a representative SHP set.

[6] In the method presented, SHPs are described by discrete probability distributions obtained by repeatedly applying PTFs to different textural compositions within a soil class. The parameter range within one soil class is then applied in a hydrologic model, and yields a discrete probability distribution of the soil moisture model output by means of ensemble forecasting. This method differs from earlier research in three ways: (1) the construction of SHP uncertainty does not rely on experimental data but on SHPs predicted with continuous PTFs for different textures within a soil class, (2) all moments of the SHP probability distribution function are determined, and (3) the interdependence of the different SHPs is taken into account. This paper aims to answer the following questions: Do region-specific and nonregion-specific PTFs generate similar SHPs and corresponding uncertainties? How are discrete SHP distributions translated into soil moisture uncertainty within a soil class? What are the implications of the simulated soil moisture distributions for data assimilation?

[7] Much attention will be given to the shape of the parameter probability distribution function (PDF), since this has been shown to have significant influence on model results [e.g., *Benke et al.*, 2008]. It should be stressed, however, that this study only focuses on uncertainty arising from textural variability within a soil class. The impact of all other sources of uncertainty involved in hydrologic modeling as discussed by *Refsgaard and Storm* [1996], including topographic data, land cover parameters, meteorological forcings, model structure, and the intrinsic uncertainty of PTFs, is outside the scope of this study. In the context of simulations in basins with unknown textural composition, it would be useful for modelers to be able to make a quick assessment of the mean system behavior within a given soil class based on one simple representative SHP set, which can be considered the best guess of the parameter values. Usually, average values for the SHP are taken from literature and considered to be representative for the soil class, without considering the geographical origin of those data. The central point of a soil class could therefore serve as a more reliable proxy to determine average SHP values for a given soil class, since this allows the use of continuous PTFs. In the literature, there is greater choice of continuous PTFs that were developed for a specific region of interest compared to class PTFs. An evaluation of the central point is carried out with respect to the representativity of the generated SHPs to reproduce the average soil moisture behavior within a given soil class.

2. Assessing the Soil Hydraulic Parameter Uncertainty

[8] The basic assumptions in this study are as follows: (1) no measurements of any soil characteristics are available, and (2) the only soil related information is a soil type map. The SHPs needed to construct the soil hydraulic model are, hence, predicted from the soil class, which was defined according to the USDA classification system. Consequently, these SHPs were subject to a high uncertainty because of lack of knowledge about the exact textural composition. It should be noted, however, that incorporation of the uncertainty in the soil type map was beyond the scope of this study.

2.1. Soil Hydraulic Model

[9] Hydrologic models require soil moisture retention curves (SMRC) and hydraulic conductivity curves (HCC) in order to express the relationship between the soil moisture content θ ($m^3\ m^{-3}$), the hydraulic head φ (m) and the hydraulic conductivity K ($m\ s^{-1}$). Within the hydrologic model that was used in this study (i.e., TOPLATS [*Famiglietti and Wood*, 1994; *Sivapalan et al.*, 1987; *Peters-Lidard et al.*, 1997a]) (see section 3.1), these relationships are given by the closed-form analytical equations of *Brooks and Corey* [1964]:

$$\begin{aligned} \theta(\phi) &= \theta_r + (\theta_s - \theta_r) \cdot \left(\frac{\phi_c}{\phi}\right)^{\lambda} \text{ if } \phi > \phi_c \\ \theta(\phi) &= \theta_s \text{ if } \phi < \phi_c \end{aligned} \tag{1}$$

$$\begin{aligned} K(\phi) &= K_s \cdot \left(\frac{\phi_c}{\phi}\right)^{2+3\lambda} \text{ if } \phi > \phi_c \\ K(\phi) &= K_s \text{ if } \phi < \phi_c \end{aligned}, \tag{2}$$

with θ_r the residual soil moisture content, θ_s the saturated soil moisture content, ϕ_c the bubbling pressure (m), λ the pore size distribution index, and K_s the saturated hydraulic conductivity. These parameters are known as the SHPs. In this study, the SHPs are predicted from basic soil properties like soil texture, bulk density, and organic matter, by means of continuous PTFs.

2.2. Prediction of SHPs Through Pedotransfer Functions

[10] Numerous pedotransfer functions for predicting SHPs have been proposed, reviewed, and evaluated over the last decade [e.g., *Tietje and Tapkenhinrichs*, 1993; *Wagner et al.*, 2001; *Nemes et al.*, 2009]. When relying on PTFs, however, modelers should be aware of the accuracy and reliability of the PTF used. The accuracy of a PTF is assessed as the correspondence between measured and predicted data for the data set from which a PTF has been developed. This is also called the intrinsic uncertainty of

the PTF and has been shown to result in substantial SHP prediction errors [e.g., *McBratney et al.*, 2002; *Minasny and McBratney*, 2002; *Soet and Stricker*, 2003]. The reliability of a PTF can be defined as the correspondence between measured and predicted data for data sets other than the one used to develop the PTF. For a detailed discussion of both characteristics, refer to *Wösten et al.* [2001].

[11] Incorporation of the intrinsic uncertainty of the PTF was beyond the scope of this study. Nevertheless, the impact of the reliability of a PTF on SHP uncertainty was evaluated by comparing two PTFs derived from data sets with different geographic origins. The PTFs of *Rawls and Brakensiek* [1985, 1989], derived from 5320 samples of 1323 soils across the U.S.A., were chosen because they are directly related to the SMRC and the HCC in the hydrologic model (equations (1) and (2)) and are very frequently used. The PTFs of *Vereecken et al.* [1989, 1990], derived from a data set of 182 horizons of 40 Belgian soils, were selected for comparison since in this study we apply the model to Belgian weather and soil conditions (see section 3.1). Considering the similarity in soil and climatic features of the region of PTF development and the region of PTF application, the *Vereecken et al.* [1989, 1990] PTFs were assumed to be more reliable for western European soils as has been demonstrated by *Cornelis et al.* [2001] and *Tietje and Tapkenhinrichs* [1993]. In this study, the PTFs of *Rawls and Brakensiek* [1985, 1989] and the PTFs of *Vereecken et al.* [1989, 1990] can therefore be referred to as nonregion-specific PTFs and region-specific PTFs, respectively.

2.2.1. PTF A: Nonregion-Specific PTF

[12] The Vereecken regression equations [*Vereecken et al.*, 1989, 1990], hereafter referred to as PTF A, were used to predict α (m^{-1}), n, θ_s, and θ_r, which are the parameters of the van Genuchten moisture retention curve [*van Genuchten*, 1980], and the saturated hydraulic conductivity K_s (Table 1). Inputs for the PTFs are the sand content, clay content, and organic carbon content (%); and bulk density (g cm^{-3}). Since no measurements were available, the organic carbon content, C, was given a realistic and constant value for Belgian soils of 1.5% [*Sleutel et al.*, 2006]. The bulk density, D (g cm^{-3}), was calculated based on the sand, clay, and organic matter content following the procedure described by *Saxton and Rawls* [2006]. With these parameters, the van Genuchten retention curve [*van Genuchten*, 1980] was constructed from which the Brooks and Corey parameters [*Brooks and Corey*, 1964], φ_c and λ, were indirectly derived by fitting the Brooks and Corey model to the van Genuchten retention curve.

[13] Since a regression is only valid for the conditions for which the relation was developed, the application of PTF A is limited to textures having a clay content $< 56.46\%$, a silt content $< 80.07\%$ and a sand content between 5.60% and 97.80% (Figure 1). One should be aware, however, that the real textural data limitations may be even more strict.

2.2.2. PTF B: Region-Specific PTF

[14] Rawls and Brakensiek [*Rawls and Brakensiek*, 1985, 1989] presented one of the few multivariate PTFs for predicting parameters of the Brooks and Corey model (equations (1) and (2)) given the sand and clay content percentages and the porosity (Table 1). The porosity, P, was calculated from the bulk density, D, and the particle density, d (%) as follows:

$$P = 1 - \frac{D}{d} \tag{3}$$

Table 1. Model Parameters and Regression Equations of the Region-Specific (PTF A) and Nonregion-Specific (PTF B) Pedotransfer Functions[a]

Model Parameters	Regression Equations
	PTF A[b]
θ_r	$0.015 + 0.005 \cdot Clay + 0.014 \cdot C$
θ_s	$0.810 - 0.283 \cdot D + 0.001 \cdot Clay$
α	$\exp(-2.486 + 0.025 \cdot Sand - 0.352 \cdot C - 2.617 \cdot D - 0.023 \cdot Clay)$
n	$\exp(0.053 - 0.009 \cdot Sand - 0.013 \cdot Clay + 0.00015 \cdot Sand^2)$
K_s	$1.1574.10^{-5} \cdot \exp(20.62 - 0.96 \cdot \ln(Clay) - 0.66 \cdot \ln(Sand) - 0.46 \cdot \ln(C) - 8.43 \cdot D)$
	PTF B[c]
φ_c	$\exp(4.34 + 0.18 \cdot Clay - 2.48\,P - 2.14 \cdot 10^{-3}\,Clay^2 - 4.36 \cdot 10^{-2}\,Sand \cdot P - 6.17 \cdot 10^{-1}\,Clay \cdot P + 1.44 \cdot 10^{-3}\,Sand^2 \cdot P^2 - 8.55 \cdot 10^{-3}\,Clay^2 \cdot P^2 - 1.28 \cdot 10^{-5}\,Sand^2 \cdot Clay + 8.95 \cdot 10^{-3}\,Clay^2 \cdot P - 7.25 \cdot 10^{-4}\,Sand^2 \cdot P + 5.4 \cdot 10^{-6}\,Clay^2 \cdot Sand + 0.50 \cdot P^2 \cdot Clay)$
λ	$\exp(0.78 + 1.76 \cdot 10^{-2}\,Sand - 1.06 \cdot P - 5.3 \cdot 10^{-5}\,Sand^2 - 2.73 \cdot 10^{-3} Clay^2 + 1.11 \cdot P^2 - 3.09 \cdot 10^{-2}\,Sand \cdot P + 2.66 \cdot 10^{-4}\,Sand^2 \cdot P^2 - 6.11 \cdot 10^{-3} Clay^2 \cdot P^2 - 2.35 \cdot 10^{-6}\,Sand \cdot Clay + 7.99 \cdot 10^{-3}\,Clay^2 \cdot P - 6.74 \cdot 10^{-3}\,P^2 \cdot Clay)$
θ_s	$1.16 \cdot 10^{-2} - 1.47 \cdot 10^{-3}\,Sand - 2.24 \cdot 10^{-3}\,Clay \cdot P + 0.98P + 9.87 \cdot 10^{-5}\,Clay^2 + 3.61 \cdot 10^{-3}\,Sand \cdot P - 1.09 \cdot 10^{-2}\,Clay \cdot P - 0.96 \cdot 10^{-4}\,Clay^2 \cdot P - 2.44 \cdot 10^{-3}\,P^2 \cdot Sand + 1.15 \cdot 10^{-2}\,P \cdot Clay$
θ_r	$-1.82 \cdot 10^{-2} + 8.73 \cdot 10^{-4}\,Sand + 5.13 \cdot 10^{-3}\,Clay + 2.94 \cdot 10^{-2}\,P - 1.54 \cdot 10^{-2}\,Clay^2 - 1.08 \cdot 10^{-3}\,Sand \cdot P - 1.82.10^{-4}\,Clay^2 \cdot P^2 + 3.07 \cdot 10^{-4}\,Clay^2 \cdot P - 2.36 \cdot 10^{-3}\,P^2 \cdot Clay$
K_s	$2.78 \cdot 10^{-6} \cdot \exp(19.52 \cdot P - 8.97 - 2.82 \cdot 10^{-2}\,Clay + 1.81 \cdot 10^{-4}\,Sand^2 - 9.41 \cdot {}^{-3}\,Clay^2 - 8.40 \cdot P^2 + 7.77 \cdot 10^{-2}\,Sand \cdot P - 2.98 \cdot 10^{-3}\,Sand^2 \cdot P^2 - 1.95 \cdot 10^{-2}\,Clay^2 \cdot P^2 + 1.73 \cdot 10^{-5}\,Sand^2 \cdot Clay + 2.73 \cdot 10^{-2}\,Clay^2 \cdot P + 1.43 \cdot 10^{-3}\,Sand^2 \cdot P - 3.5 \cdot 10^{-6}\,Clay^2 \cdot Sand)$

[a] θ_s is the saturated soil moisture content ($m^3\ m^{-3}$), θ_r the residual soil-moisture content ($m^3\ m^{-3}$), K_s the saturated hydraulic conductivity (cm s^{-1}), λ the pore size distribution, φ_c the bubbling pressure (cm), α is a van Genuchten parameter and is related to the inverse of the air entry suction (cm^{-1}), n is a van Genuchten parameter and is a measure of the pore size distribution, D the bulk density (g cm^{-3}), C the organic carbon content (%), *Clay* the clay content (%), *Sand* the sand content (%), and P the porosity.

[b] *Vereecken et al.* [1989, 1990].

[c] *Rawls and Brakensiek* [1985, 1989].

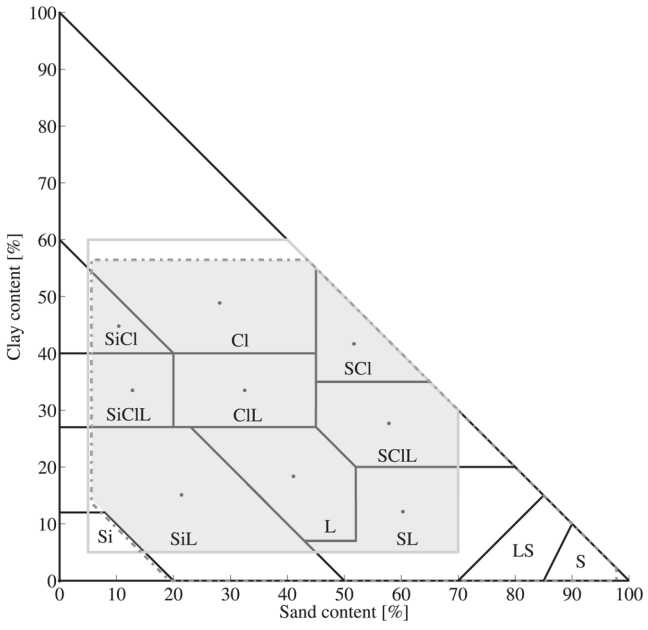

Figure 1. USDA texture triangle with indication of the boundary conditions on the PTFs of *Rawls and Brakensiek* [1985, 1989] (gray full line) and on the PTFs of *Vereecken et al.* [1989, 1990] (gray dashed line); the area of the particle size distributions considered in the study is shaded and the central point per soil class is indicated with a gray dot.

[15] The particle density, d, was corrected for the organic matter content, for which a density of 1.4×10^{-3} [g/cm^{-3}] [*Kaiser and Guggenberger*, 2003; *Mayer et al.*, 2004] was assumed. The bulk density, D, was calculated following the procedure as described by *Saxton and Rawls* [2006]. Application of the *Rawls and Brakensiek* [1985, 1989] PTFs is limited to textures with clay and sand contents of 5–60% and 5–70%, respectively (Figure 1). For the remainder of this paper, the Rawls and Brakensiek model is referred to as PTF B.

[16] Since both PTFs A and B were applied, all calculations are restricted to the overlapping validity range as shown by the shaded area in Figure 1. The soil class silt (Si) was excluded from the calculations because the area satisfying the limits on validity of the PTFs was very small. Other classes were also truncated, but because a considerable portion of the class was still covered they were included in the study; the results only apply for the areas covered by the overlap. The USDA texture classes that were considered in this study are silty clay (SiCl), clay (Cl), silty clay loam (SiClL), clay loam (ClL), sandy clay (SCl), sandy clay loam (SClL), sandy loam (SL), loam (L), and silt loam (SiL).

Table 2. Number of Synthetically Generated Samples in the Nine Truncated USDA Soil Classes Considered

Texture Class	Samples
SL	328
SClL	373
SCl	231
L	392
ClL	364
SiL	622
SiClL	210
SiCl	106
Cl	574

2.3. Within-Soil-Class Variability of SHPs

[17] Each soil class contains a range of particle size distributions, given by its sand (2–0.05 mm), silt (0.05–0.002 mm), and clay (< 0.002 mm) content, hence, within a soil class, the SHPs are variable. In order to account for this variability, the USDA texture triangle was uniformly sampled along a regular grid with a spacing of 1%, excluding the samples that fall outside the valid area for PTF application (Figure 1). The resulting number of samples per soil class is given in Table 2. The SHPs for each sample were predicted with either PTF A or PTF B, resulting in a discrete probability distribution of each SHP per soil class, which was characterized by its first four moments (mean, variance, skewness, and kurtosis). The set of SHPs obtained with PTF A and PTF B are referenced as respectively, SHPs-A and SHPs-B.

2.3.1. Mean and Standard Deviation

[18] The mean SHPs-A and SHPs-B for each soil class are given in Tables 3 and 4 together with the corresponding standard deviation, σ_{unit}, which is expressed per unit area on the texture triangle (defined as a square with a range of 1% clay and 1% sand) in order to avoid poor standard deviation statistics by truncating the soil class. For θ_r and φ_c, PTF A gives consistently higher values in comparison to PTF B, while for λ the opposite is observed. For θ_s and K_s, differences between PTF A and PTF B are inconsistent. Likewise, the standard deviation of the SHPs within a soil class seems to be highly dependent on the PTF used. In general, PTF B results in larger standard deviations (Tables 3 and 4). These findings demonstrate the large disagreements in predicted SHPs between different PTFs, as was already reported by *Soet and Stricker* [2003], *Cornelis et al.* [2001], and others.

[19] Figure 2 illustrates the relation between the textural composition and the predicted K_s and φ_c. From Figure 2, it can be seen that both SHPs are affected by texture in

Table 3. Mean and SD per Unit Area on the USDA Texture Triangle of the SHPs Predicted From PTF A for the Nine Selected Soil Classes

Texture	θ_s ($m^3\ m^{-3}$)		θ_r ($m^3\ m^{-3}$)		φ_c (m)		λ		K_s ($m\ day^{-1}$)	
	μ	σ_{unit}	μ	σ_{unit}	μ	σ_{unit}	μ	σ_{unit}	μ	σ_{unit}
SL	0.45	1.16E-05	0.12	8.87E-05	0.27	1.13E-04	0.69	7.27E-04	0.28	7.03E-04
SClL	0.46	2.52E-05	0.20	6.56E-05	0.20	8.13E-05	0.28	1.82E-04	0.07	6.89E-05
SCl	0.48	5.59E-05	0.27	1.27E-04	0.24	3.18E-04	0.15	1.42E-04	0.05	5.84E-05
L	0.47	2.73E-05	0.15	8.04E-05	0.3	9.30E-05	0.46	4.14E-04	0.26	2.88E-04
ClL	0.49	3.44E-05	0.22	6.21E-05	0.36	2.39E-04	0.22	1.14E-04	0.20	2.81E-04
SiL	0.48	2.46E-05	0.13	5.50E-05	0.45	1.40E-04	0.57	3.02E-04	0.93	8.39E-04
SiClL	0.52	4.95E-05	0.22	1.08E-04	0.61	4.74E-04	0.25	2.15E-04	0.78	1.80E-03
SiCl	0.54	1.06E-04	0.28	1.76E-04	0.94	2.30E-03	0.17	1.94E-04	0.88	3.1E-03
Cl	0.52	3.69E-05	0.30	4.44E-05	0.73	6.66E-04	0.14	4.32E-05	0.26	4.34E-04

different ways, with large differences between the results of the two PTFs. Depending on the soil class, the within-soil-class variability of K_s and φ_c is dominated by a variation in either the sand or clay content. Sensitivity of the SHPs to those variations is indicated by the density of the contour lines. As can be seen from Figure 2, the sensitivity toward texture of the SHPs largely depends on the choice of PTF. In general, an increase in sensitivity can be observed with increasing clay content. The differences in variability and sensitivity of the SHPs in relation to soil texture can be attributed to differences in geographic origin of the data sets used to construct the PTFs, since the origin determines the soil and climatic conditions (see section 2.2). Furthermore, the information content of both datasets may differ with respect to the number of soil samples, the variability in sampled textures, the methods used to measure the SHPs, etc. These differences are reflected in the resulting regression equation (Table 1) and continue to exist in the behavior of the SHPs in relation to soil texture. For example, θ_s and θ_r are insensitive to sand content, according to PTF A, whereas, in PTF B, the same parameters vary with the sand content. This raises questions about the general applicability of the standard PTFs (often nonregion specific) as it seems that a crucial soil variable (e.g., soil structure) to allow for nonregion-specific application is missing in the regression.

2.3.2. Shape of the Parameter Probability Density Function

[20] Skewness (Skew) and kurtosis (Kurt), the third-and fourth-order moments, respectively, characterize the shape of a probability density function. The former is a measure of the asymmetry, whereas the latter is a measure for the peakedness of the distribution. In case skewness is absent (Skew = 0), the distribution is symmetric. A positive (negative) skewness indicates the presence of a long right (left) tail, so few high (low) values are included. A distribution is said to be Gaussian or normal if both the skewness and the kurtosis (the latter with a correction of −3) are zero.

[21] Both characteristics were calculated for each SHP PDF and are listed in Tables 5 and 6 for PTFs A and B, respectively. From these tables, it can be seen that the PDF of most SHPs does not represent a normal distribution. Assuming a normal or lognormal distribution (i.e., only defining the first 2 moments) for the SHPs would therefore imply a loss of information. It seems that the shape of the PDF is not only a function of the SHP itself, but also depends on the soil class and choice of PTF. This is illustrated in Figure 3, showing the PDF of K_s and φ_c for the soil class ClL. This class is chosen because of its central position on the soil texture triangle (no extreme textures). It is clear that the PTFs result in both a different range of SHP values and a different shape of the SHP distribution. Therefore, it can be stated that the selection of PTF is a crucial step in assessing the uncertainty in the SHPs. If region-specific PTFs are available, they are preferable since they are assumed to generate more reliable SHPs than nonregion-specific PTFs. Furthermore, the higher-order moments are required to accurately describe the SHP PDF, since assuming a normal distribution may not be representative for the SHP at hand.

3. Modeling the Impact of Soil Hydraulic Parameter Uncertainty on Hydrologic Model Predictions

[22] The constructed discrete probability distributions of the SHPs were used to generate a number of hydrologic

Table 4. Mean and SD per Unit Area on the USDA Texture Triangle of the SHPs Predicted From PTF B for the Nine Selected Soil Classes

Texture	θ_s ($m^3\ m^{-3}$)		θ_r ($m^3\ m^{-3}$)		φ_c (m)		λ		K_s ($m\ day^{-1}$)	
	μ	σ_{unit}	μ	σ_{unit}	μ	σ_{unit}	μ	σ_{unit}	μ	σ_{unit}
SL	0.44	3.49E-05	0.07	6.35E-05	0.13	1.29E-04	1.79	5.54E-04	0.97	1.70E-03
SClL	0.44	4.51E-05	0.10	2.12E-05	0.13	1.28E-04	1.22	5.14E-04	0.47	1.00E-03
SCl	0.49	1.34E-04	0.11	7.32E-06	0.19	2.82E-04	0.76	6.98E-04	0.08	3.30E-04
L	0.46	3.61E-05	0.08	4.26E-05	0.24	1.67E-04	1.58	4.53E-04	0.22	3.35E-04
ClL	0.50	5.55E-05	0.10	1.71E-05	0.36	2.61E-04	1.15	3.83E-04	0.05	7.64E-05
SiL	0.49	2.84E-05	0.06	3.20E-05	0.41	1.53E-04	1.62	2.34E-04	0.10	1.07E-04
SiClL	0.54	7.89E-05	0.10	3.40E-05	0.56	2.47E-04	1.23	4.84E-04	0.03	3.29E-05
SiCl	0.58	1.89E-04	0.11	2.38E-05	0.67	5.06E-04	1.00	6.22E-04	0.01	2.48E-05
Cl	0.57	5.92E-05	0.11	3.44E-06	0.53	2.79E-04	0.78	2.43E-04	0.02	1.44E-05

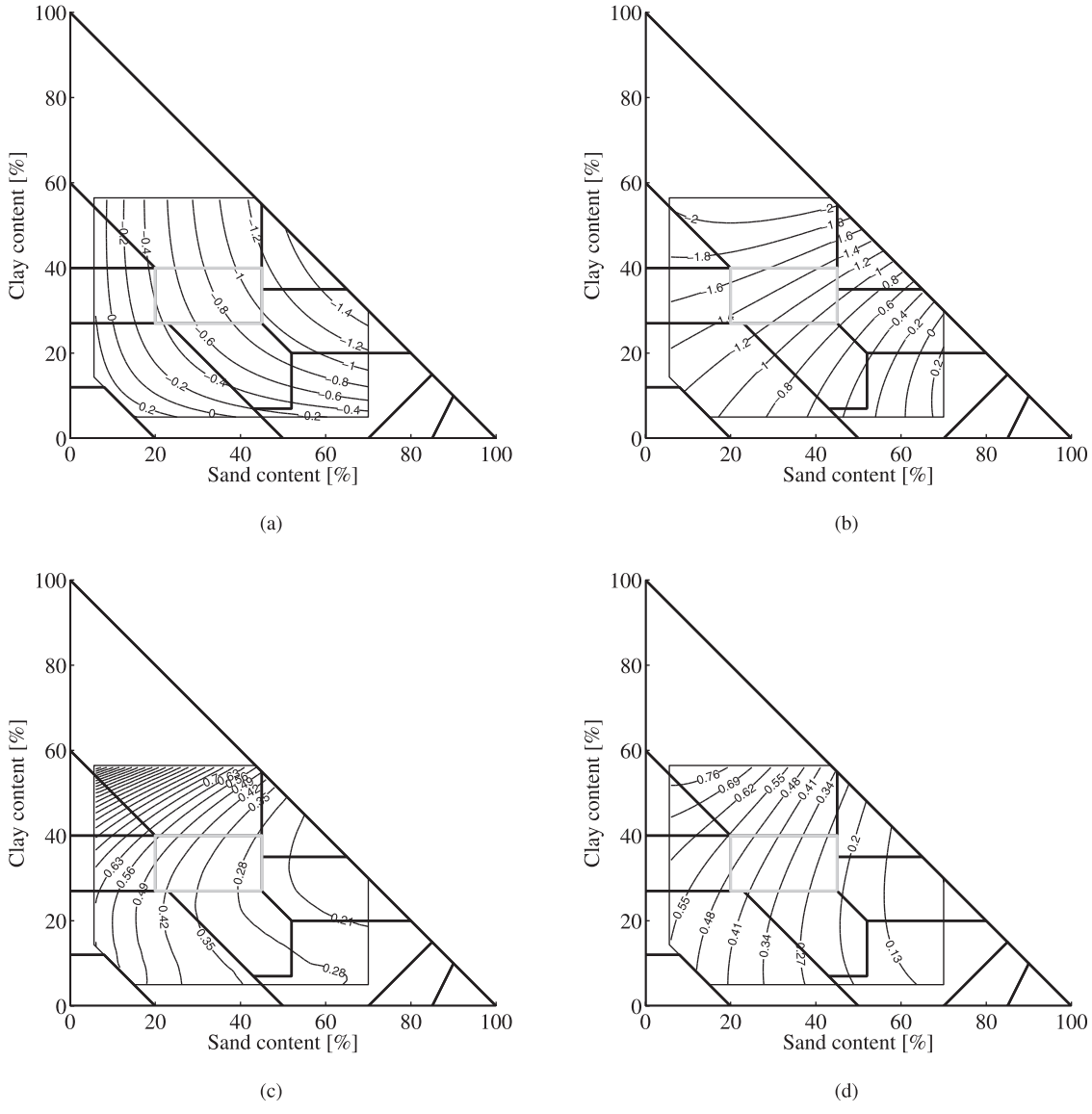

Figure 2. (top) Contour plot of the logarithm (log10) of the saturated hydraulic conductivity K_s predicted with (a) PTF A and (b) PTF B. (bottom) Contour plot of the bubbling pressure φ_c predicted with (c) PTF A and (d) PTF B. The soil class clay loam is highlighted in gray.

model forecasts (equal to the number of texture samples given in Table 2) by drawing a combination of parameters from the distributions, on the basis of random sampling. The SHP PDFs were not sampled individually to preserve the correlation between SHPs. We evaluated how the shape of the SHP PDF translated into the PDF of modeled soil moisture. We compared model prediction uncertainties resulting from SHPs-A and SHPs-B.

Table 5. Skewness and Kurtosis of the SHPs Predicted From PTF A for the Nine Selected Soil Classes of the USDA Texture Triangle

	θ_s ($m^3\ m^{-3}$)		θ_r ($m^3\ m^{-3}$)		φ_c (m)		λ		K_s ($m\ day^{-1}$)	
Texture	Skew	Kurt	Skew	Kurt	Skew	Kurt	Skew	Kurt	Skew	Kurt
SL	−0.10	−0.59	0.11	−1.27	0.12	−0.36	0.19	−1.21	1.09	0.20
SClL	0.32	−0.79	−0.05	−1.11	−0.13	−0.94	0.49	−0.82	0.38	−0.73
SCl	0.07	−0.58	0.57	−0.61	1.17	1.62	−0.23	−0.99	0.52	−0.32
L	0.64	−0.43	−0.27	−1.00	0.46	0.31	0.88	−0.17	0.97	0.84
ClL	0.18	−0.74	4.55E-14	−1.21	0.46	−0.67	0.24	−1.05	0.68	−0.53
SiL	0.30	−0.86	0.18	−1.08	0.37	−0.93	0.29	−1.08	0.96	0.19
SiClL	0.13	−0.63	3.63E-14	−1.21	0.42	−0.40	0.25	−1.04	0.78	−0.43
SiCl	0.18	−0.60	0.57	−0.62	1.00	0.74	−0.28	−0.81	0.27	−1.07
Cl	0.37	−0.63	−0.17	−1.16	1.17	0.88	0.28	−0.89	2.19	5.72

Table 6. Skewness and Kurtosis of the SHPs Predicted From PTF B for the Nine Selected Soil Classes of the USDA Texture Triangle

	θ_s (m^3 m^{-3})		θ_r (m^3 m^{-3})		φ_c (m)		λ		K_s (m day^{-1})	
Texture	Skew	Kurt	Skew	Kurt	Skew	Kurt	Skew	Kurt	Skew	Kurt
SL	0.01	−0.55	−0.11	−1.23	0.63	0.08	−0.29	−1.10	0.62	−0.71
SClL	0.28	−0.73	−0.42	−0.85	0.42	−0.841	2.40E-03	−1.06	1.26	1.04
SCl	0.51	−0.32	−1.32	1.18	0.14	−0.68	−0.16	−0.91	1.58	2.67
L	0.80	−0.05	−0.59	−0.68	0.78	−0.06	0.20	−1.08	0.65	−0.50
ClL	0.12	−0.62	−0.43	−0.85	0.12	−1.08	−0.15	−0.97	1.21	1.20
SiL	0.31	−0.70	−0.06	−1.11	−0.08	−0.94	−0.10	−0.94	1.52	2.23
SiClL	0.12	−0.73	−0.27	−1.11	−0.14	−0.74	−0.06	−1.15	0.53	−0.49
SiCl	0.43	−0.51	0.12	−1.07	−0.03	−0.49	−0.30	−0.81	0.01	−0.99
Cl	0.10	−0.75	−0.39	0.82	0.09	−1.08	−0.31	−0.60	1.52	2.34

3.1. Hydrologic Model and Data Description

[23] The hydrologic model used in this study is TOPLATS, the TOPMODEL-Based Land-Atmosphere Transfer Scheme [*Famiglietti and Wood*, 1994; *Sivapalan et al.*, 1987; *Peters-Lidard et al.*, 1997]. TOPLATS was run at the point scale on coordinates 50.89°N and 4.09°E, for which bare soil conditions were assumed. For this location, the soil corresponds to the USDA class L. The texture, however, was not fixed but was varied within the simulation experiment. Belgian weather conditions were considered: a temperate climate with an annual mean temperature of 11.5 °C and a total annual rainfall of 750 mm, quite uniformly distributed throughout the year. In order to run the hydrologic model, a set of meteorological variables, measured at a nearby meteorological station during the year 2006, was used. The SHPs were derived following the methodology described in section 2.2. The vegetation parameters were determined from the land cover classification (in this case bare soil) following *Peters-Lidard et al.* [1997] and the base flow parameters were taken from *Samain et al.* [2011]. The simulated soil moisture content for the upper soil layer (5 cm) was validated with in situ soil moisture measurements taken at the simulation point at 2.5 cm depth between May 13 and May 30, 2007 (not shown).

3.2. Modeling Prediction Uncertainty Through Ensemble Forecasting

[24] In order to assess uncertainty in the model states or model output, an ensemble of model runs was performed, for which each ensemble member differed from other members only in its SHPs. Such an ensemble was constructed for each selected USDA soil class (see section 2.2) by attributing the SHPs of each texture sample within the soil class (see Table 2) to the point for which TOPLATS was run. Each model run resulted in a time series of simulated daily soil moisture content, θ_{daily}, within the upper 5 cm of the soil. The procedure was performed using SHPs-A and SHPs-B. This resulted in two different ensembles of θ_{daily} per soil class, and is illustrated in Figure 4 with a spaghetti plot of the different ensemble members for the classes SL (328 ensemble members) and SiCl (106 ensemble members). These two classes were chosen since they represent two extremes on the texture triangle (Figure 1). A window of 70 days, starting from day of year (DOY) 200 (i.e., 19 July) up to DOY 270 (i.e., 27 September), was selected to properly visualize the behavior of each ensemble member.

[25] From Figure 4, it can be seen that (1) there is a substantial impact of within-soil-class variability of SHPs on the modeled soil moisture and (2) there are large differences with respect to the predicted value, the dynamics, and

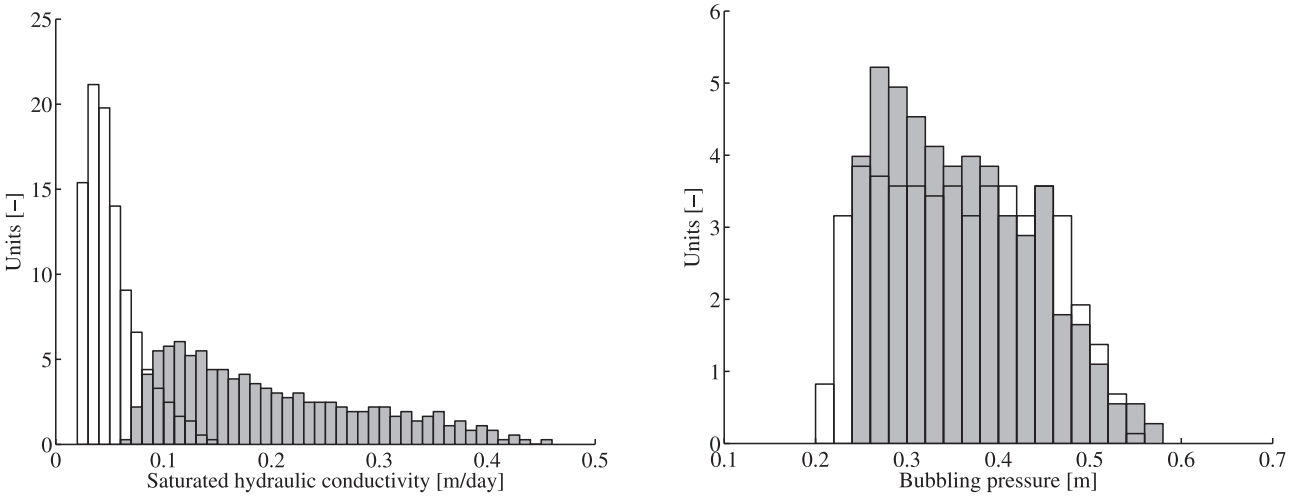

(a) (b)

Figure 3. Probability distribution of (a) the saturated hydraulic conductivity, K_s, and (b) the bubbling pressure φ_c, predicted with PTF A (gray) and PTF B (white) for the soil class clay loam.

the range of the ensembles between PTFs A and B. For the soil class SL it is apparent that all ensemble members resulting from SHPs-B predict lower soil moisture values than those resulting from SHPs-A. Additionally, the use of SHPs-B results in a much higher density of ensemble members, whereas SHPs-A produce a more uniform distribution of the ensemble members. The PTF also affects the dynamics in the predicted soil moisture, as can be seen from the spaghetti plot of SiCl (Figure 4). Despite better correspondence in average simulated soil moisture, SHPs-B cause a faster wetting and drying of the soil as compared to the dynamic in θ_{daily} resulting from SHPs-A. The intensity of fluctuations in soil moisture is related to the shape of the SMRC and the HCC (see section 2.1). For each set of SHPs in the ensemble, both curves were constructed and are shown in Figure 5. It is clear that the SMRC is more nonlinear for SHPs-B than for SHPs-A. The difference in SMRC between the region- and nonregion-specific PTFs is most apparent for SiCl (mainly because of the discrepancy in θ_r, Tables 3 and 4).

[26] All ensemble members were averaged in time in order to obtain a single value per PTF application, referred to as the average simulated soil moisture content θ_{avg}, for each sample on the texture triangle. This model output was

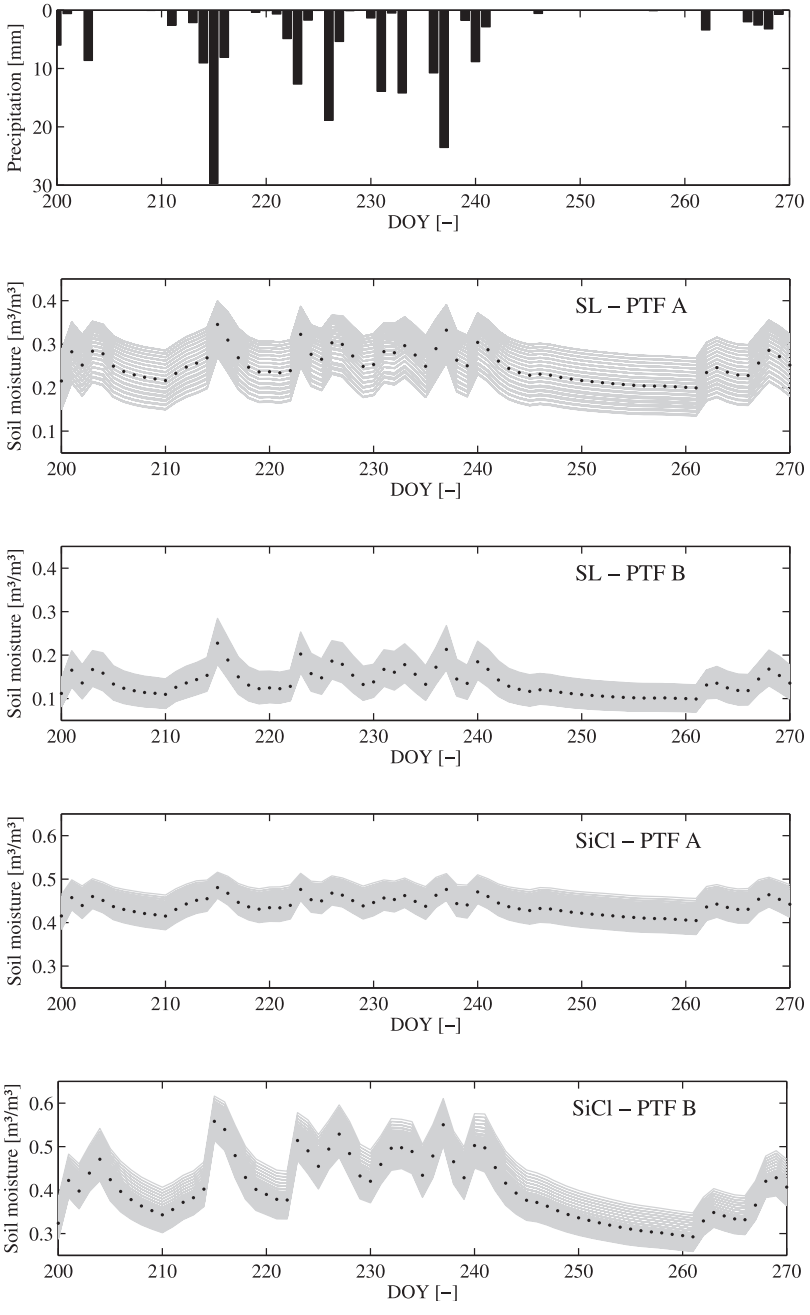

Figure 4. Spaghetti plots of the 2006 daily simulated soil-moisture content, θ_{daily}, for sandy loam (SL) and silty clay (SiCl) with the SHPs predicted from PTF A and PTF B; the ensemble mean is indicated with black dots.

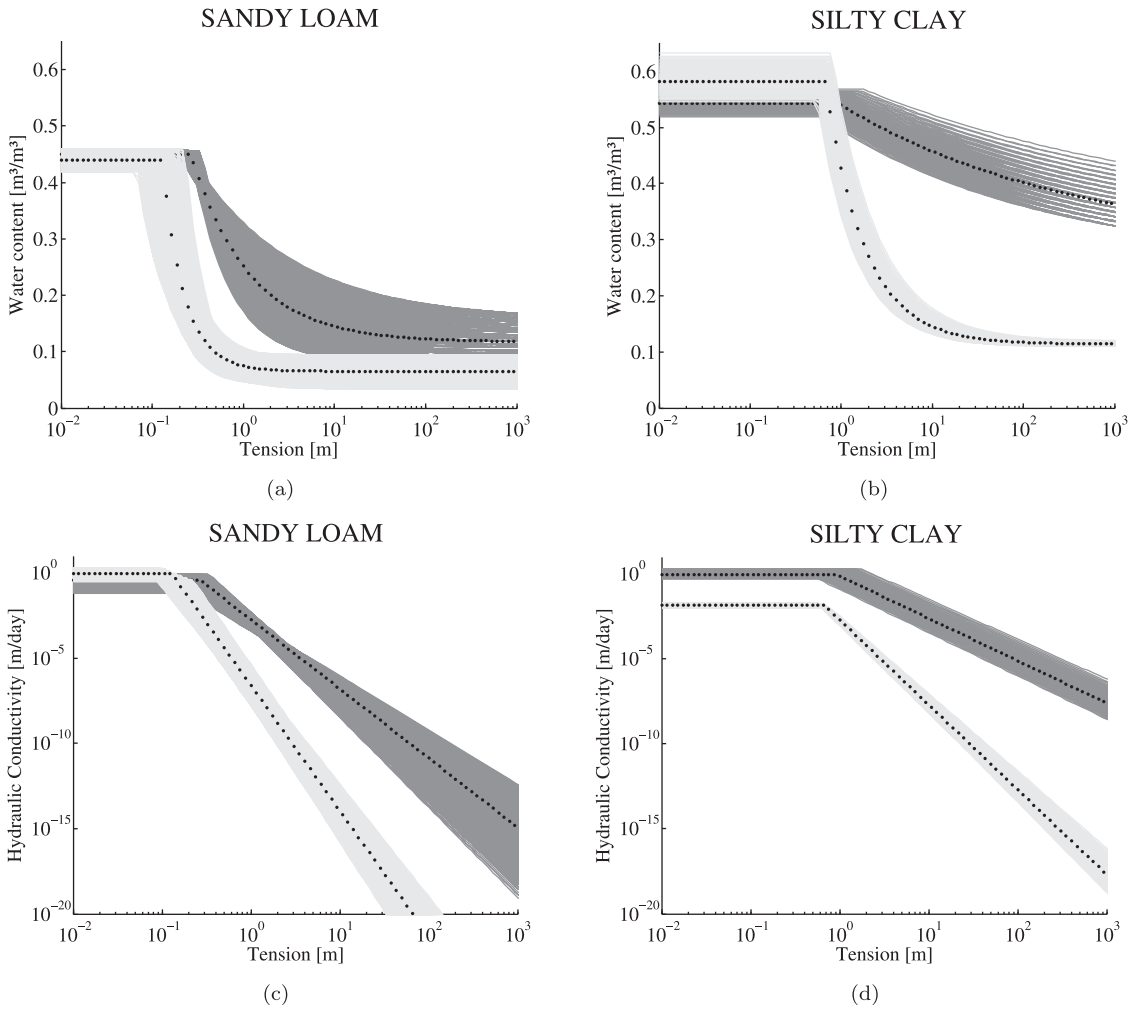

Figure 5. (left) Ensemble (328 members) of (a) soil-moisture retention curves and (c) hydraulic conductivity curves, for the soil class sandy loam resulting from application of PTF A (dark gray) and PTF B (light gray). (right) Ensemble (106 members) of (b) soil-moisture retention curves and (d) hydraulic conductivity curves, for the soil class silty clay resulting from application of PTF A (dark gray) and PTF B (light gray). Ensemble means are indicated with black dots.

projected on the texture triangle, resulting in a contour plot as shown in Figure 6. In this way, the sensitivity of the model output to soil texture, as a result of the joint sensitivity of the SHPs to texture, was deduced. As can be seen from Figure 6, θ_{avg} resulting from SHPs-A decreases with decreasing clay content and is nearly unaffected by the sand content. When using SHPs-B, however, both a decrease in clay content and an increase in sand content cause a reduction of θ_{avg}. From the density in contour lines, it can be derived that the within-soil-class variability of θ_{avg} increases for a decreasing clay content for SHPs-A, whereas the opposite is observed when using SHPs-B. These results reflect the empirical relationships between the SHPs and textural composition (Table 1). For example, the insensitivity of θ_s and θ_r to sand content determines the dominant influence of clay content on simulated soil moisture in PTF A.

3.2.1. Ensemble Statistics

[27] The statistics of the ensembles of θ_{daily} were further analyzed through their moments. The first four moments of a PDF at day i are given by the ensemble mean, $Mean_i$; the ensemble variance or spread, $Spread_i$; the skewness, $Skew_i$; and the kurtosis, $Kurt_i$.

3.2.2. Mean and Spread

[28] The temporal behavior of the ensemble mean and the ensemble spread for θ_{daily} is illustrated for the classes SL and SiCl in Figure 7, which clearly demonstrates the impact of the PTF on fluctuations in mean predicted soil moisture. As explained earlier, these differences in fluctuation can be attributed to the different shapes of the SMRCs (see Figure 5). The evolution of the ensemble spread is also affected by the choice of PTF, but its extent depends on the soil class considered. Fluctuations in both the ensemble mean and spread are closely related to the precipitation regime. When rainfall events occur, water tension decreases and eventually drops below the bubbling pressure. When $\varphi = \varphi_c$, a turning point is clearly visible in both the SMRC and HCC (Figure 5). At this point, the soil moisture equals θ_s and the hydraulic conductivity is K_s. If $\varphi < \varphi_c$, there is substantially less spread in HCC than there is when $\varphi > \varphi_c$. A rainfall event is therefore generally accompanied with a decrease in ensemble spread.

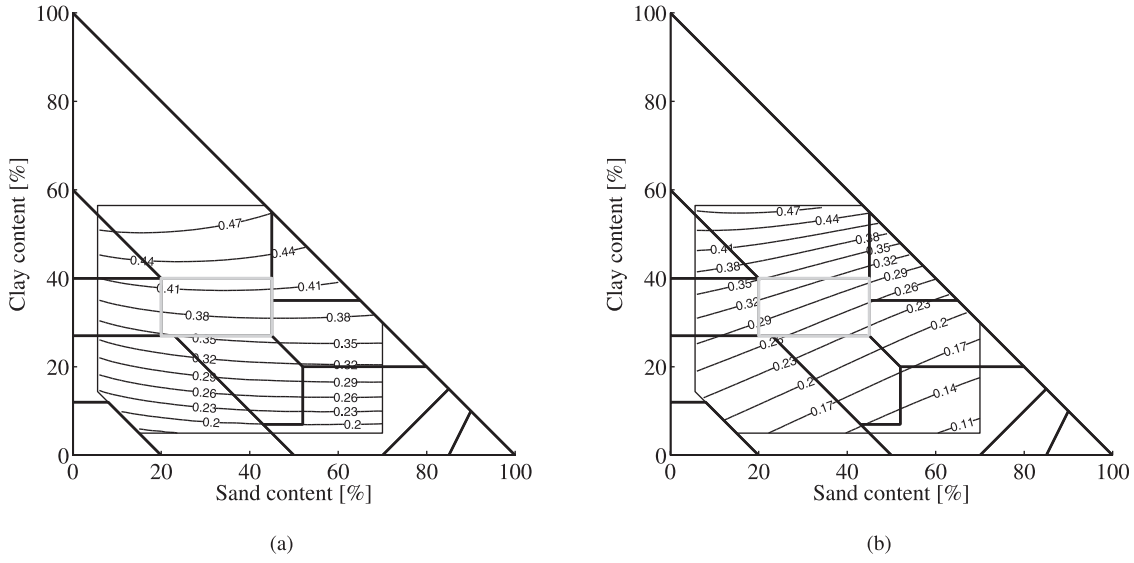

Figure 6. Contour plot of the average simulated soil-moisture content, θ_{avg}, using the SHPs predicted from (a) PTF A and(b) PTF B. The soil class clay loam is highlighted in gray.

[29] For θ_{avg}, the mean and standard deviation per unit area on the texture triangle were calculated for each soil class and are listed in Table 7. Table 7 shows that θ_{avg} obtained with SHPs-A are consistently higher than when SHPs-B were used. Nevertheless, the differences are smallest for the soil classes with low sand content (SiL, SiClL, SiCl, and Cl). In general, the standard deviation of θ_{avg} is slightly higher when SHPs were predicted with PTF B. This could be expected because of the higher standard deviation associated with SHPs-B compared to SHPs-A (see section 2.3.1). The consistent underestimation of soil moisture obtained with the nonregion-specific PTF (PTF B) as compared to the region-specific PTF (PTF A), indicates that this is not purely by chance. It can therefore be argued that there is a fundamental difference between the region- and nonregion-specific PTFs.

3.2.3. Skewness and Kurtosis

[30] As mentioned in section 2, the skewness and kurtosis characterize the shape of a distribution. The evolution of both statistics in time for θ_{daily} can be found in Figure 7. It can be seen that often there is wide variation in the shape of the PDF through time, but the evolution over time depends on the PTF used and on the soil class considered. In general, the distribution deviates from normality with either a too flat or too skewed distribution. The evolution in PDF shape can be linked to the precipitation regime but fluctuations are not always as wide as those in the ensemble mean. For the SiCl soil, skewness and kurtosis are more stable than for the SL soil; this implies a steadier evolution of the soil-moisture distribution. A possible explanation for this can be found in the shape of the HCC, which is less nonlinear for SiCl than for SL (Figure 5).

[31] The skewness and kurtosis for θ_{avg} are given in Table 7, for the model run with both SHPs-A and SHPs-B. From these values, it can be seen that when using SHPs-B the distribution of θ_{avg} tends to result in a positively skewed and flattened distribution, whereas for SHPs-A the distribution is either positively or negatively skewed depending on the soil class. Figure 8 shows the discrete distribution of θ_{avg} for the soil class ClL (highlighted in Figure 6). This class is chosen because of its central position on the texture triangle (no extreme textures). It can be seen that the choice of PTF for predicting the SHPs has a substantial impact on (1) the absolute value of the predicted soil moisture, (2) the range of simulated soil moisture, and (3) the shape of the soil-moisture distribution. Selecting the most reliable PTF is therefore a crucial step when assessing the uncertainty in the modeled soil moisture since differences between region- and nonregion-specific PTFs remain after propagating the SHP PDFs through the hydrologic model.

3.3. Implications for Data Assimilation

[32] The aforementioned findings provide some suggestions for data assimilation applications. State estimation through data assimilation typically assumes Gaussian forecast errors. However, as can be observed from Figure 7, the state variable θ_{daily} is nonnormally distributed throughout the entire simulation period. In addition, because of the nonlinear behavior of the system, fluctuations in the shape of the state's PDF occur when propagating through the model, especially when rain events or long drought periods occur. Suppose that the state's PDF is approximated by a normal distribution; much of the information on the modeled state would be lost since the PDF cannot be fully represented by its mean and variance. This is illustrated in Figure 9, which shows the probability distribution of θ_{daily} in a SiCl soil on a wet day (DOY 215) and on a dry day (DOY 260). The corresponding normal distribution is plotted on top of the empirical distribution. From Figure 9, it can be seen that, because of the skewness, the density in low soil-moisture values is underestimated when assuming a normal distribution, especially when dealing with dry conditions. Nevertheless, it is difficult to generalize the impact of the Gaussian error assumption considering the profound influence of the parameter prediction method on model output distribution. Consequently, nonlinear filters accounting for nonnormal

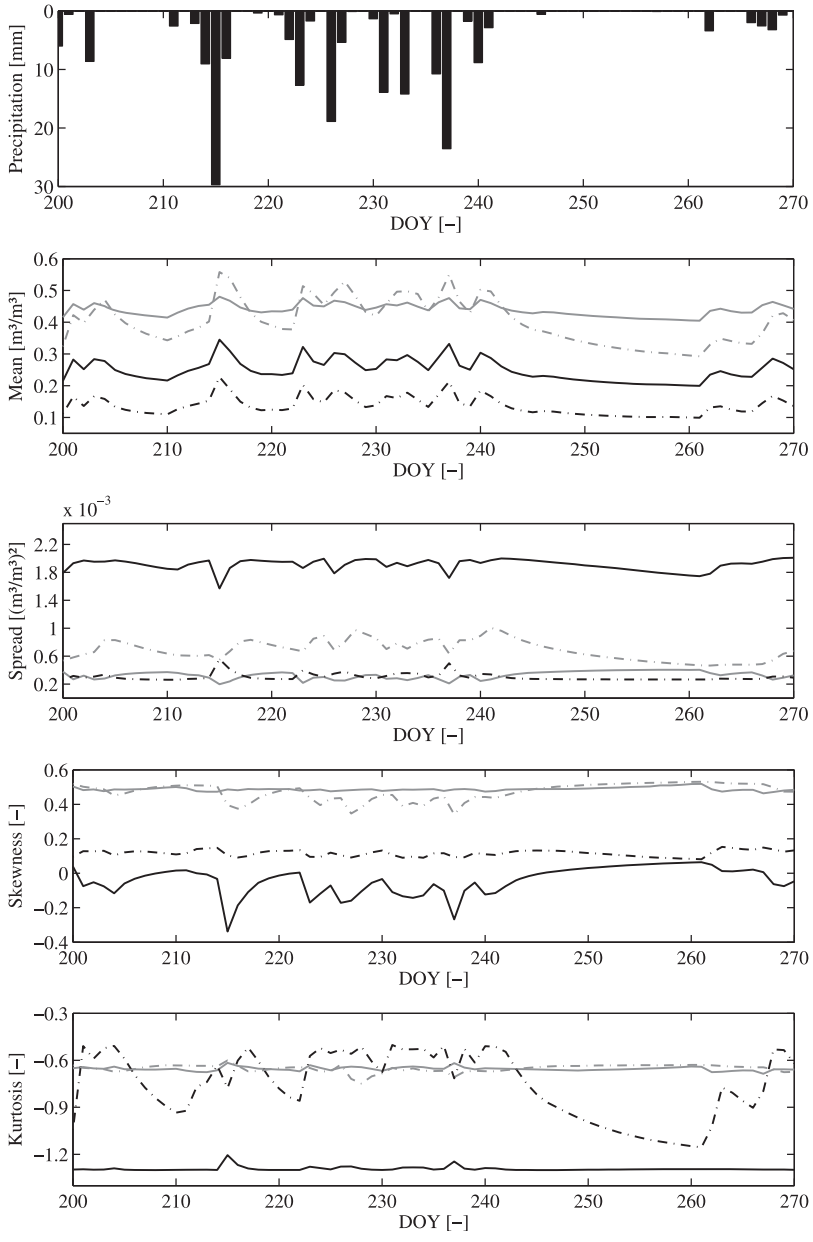

Figure 7. Time series of the ensemble mean, spread, skewness, and kurtosis for the 2006 simulated soil-moisture content, θ_{daily}. Results are given for the soil classes sandy loam (black) and silty clay (gray) using the SHPs predicted from PTF A (solid line) and PTF B (dotted line).

distributions and nonlinear systems should be used. Applying methods that rely on normal error assumptions may compromise the performance of the assimilation algorithm in such cases.

4. Evaluation of the Central Point as a Proxy for Soil Class

[33] We examined whether the central point (CP), corresponding to the center of gravity of a soil class, could serve as a representative point from which to (1) generate a best guess SHP set and (2) generate the average behavior in modeled soil moisture content. The resulting SHPs and modeled soil moisture were compared to the common practice of using average soil class SHPs from literature.

4.1. Representative Soil Hydraulic Parameters

[34] For each of the nine selected soil classes, the CP was determined with respect to the limits on the PTFs (Figure 1). The textural information of the CP was used as input for PTFs A and B, which resulted in two sets of SHPs (Figure 10). These SHPs were compared to the mean predicted SHPs of the corresponding soil class (as can be found in Tables 3 and 4). Given their close correlations (not shown), the CPs can be considered good proxies for the average SHPs per soil class. Furthermore, the SHPs of the CPs are mostly located near the center of the total range in predicted SHPs. In order to assess the impact of PTF limits on performance of the CP, the CPs corresponding to the full area of the soil classes falling partly or completely outside

Table 7. Mean, SD per Unit Area on the Texture Triangle, Skewness, and Kurtosis of the Average Simulated Soil-Moisture Content[a] for the Nine Selected USDA Classes Using the SHPs Predicted From PTF A and PTF B[a]

Texture	θ_{avg} ($m^3\ m^{-3}$) With SHPs From PTF A				θ_{avg} ($m^3\ m^{-3}$) With SHPs From PTF B			
	μ	σ_{unit}	Skew	Kurt	μ	σ_{unit}	Skew	Kurt
SL	0.25	1.644E-04	−0.03	−1.30	0.13	6.24E-05	0.13	−0.68
SClL	0.36	6.96E-05	−0.26	−1.02	0.20	7.79E-05	0.25	−0.78
SCl	0.42	9.53E-05	0.48	−0.72	0.30	2.51E-04	0.71	−0.22
L	0.30	1.22E-04	−0.52	−0.77	0.19	9.31E-05	0.16	−0.88
ClL	0.39	6.48E-05	−0.14	−1.15	0.28	9.26E-05	0.07	−0.73
SiL	0.25	8.54E-05	0.05	−1.11	0.21	6.83E-05	0.07	−0.93
SiClL	0.38	1.33E-04	−0.12	−1.10	0.32	1.32E-04	0.02	−1.03
SiCl	0.44	1.76E-04	0.49	−0.66	0.40	2.53E-04	0.48	−0.65
Cl	0.46	3.79E-05	−0.10	−1.05	0.40	8.63E-05	−0.22	−1.01

[a]Within the upper 5 cm of the soil during the year 2006.

the valid area on the texture triangle were determined. The corresponding SHPs were calculated and compared to the mean SHPs of the full soil class. Again, the CP was found to be representative for the soil class (not shown), from which it can be assumed that irrespective of the area on the texture triangle covered by the soil class, the CP performs well to generate a representative set of SHPs. Nevertheless, one should be aware that because of the complexity and the nonlinearities in the relationships between the SHPs and soil texture, the CP may not correspond to the real central point in terms of hydraulic properties.

[35] An alternative and more common way to determine a best guess SHP set is to take average values from literature. Frequently used literature values are those reported by *Rawls et al.* [1982] and *Meyer et al.* [1997] (based on data sets from the United States); these are shown in Figure 10. From Figure 10, it can be seen that the literature values often fall outside the range of SHPs predicted with the continuous PTFs; for θ_s especially there is a large deviation. For some SHPs, like θ_r and K_s, the literature values agree more with SHPs-B than with SHPs-A, while for other parameters, like λ, the opposite is observed. Also note the significant disagreement among the literature sources themselves, for example, in the value of K_s for SiCl. These observed differences highlight the relevance of the reliability of continuous and class PTFs for determining a representative set of SHPs. In this context, the CP can serve as a tool to construct a more reliable average set of SHPs than those derived from class PTFs. In literature, there is a wider choice of continuous PTFs compared to class PTFs. Most PTFs that were developed for a specific region are continuous.

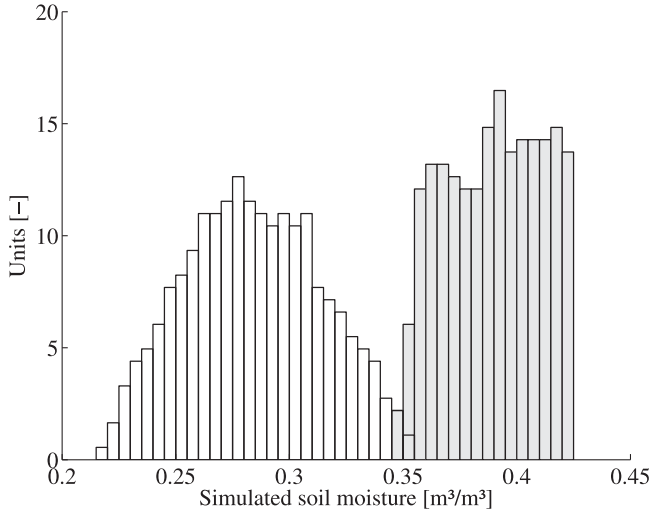

Figure 8. Probability distribution of the average simulated soil-moisture content, θ_{avg}, using the SHPs predicted from PTF A (gray) and PTF B (white) for the USDA soil class clay loam.

4.2. Average Soil Moisture Behavior

[36] TOPLATS was run with the two parameter sets of the CP, as obtained from PTFs A and B. The resulting average soil-moisture content, θ_{avg}, is shown in Figure 10 and was compared to the mean prediction of θ_{avg} from Table 7. This comparison pointed out that the CP is a good proxy for the mean θ_{avg} within a given soil class. From Figure 10, it can be seen that the model output with the CP tends to be situated near the central part of the total range of model outputs. For the CP of the classes SiL, SiClL, SiCl, and Cl, the difference in generated soil moisture between the region- and nonregion-specific PTFs is relatively small given the large difference in their predicted SHPs. For the other classes, the discrepancy between both model outputs is large, with only a small overlap in the range of predicted soil moisture. The average simulated soil moistures obtained with the literature-based SHPs are also shown in Figure 10. By analogy with the CP, it can be said that in contrast to the huge differences in SHPs, the differences in model output are minor. For many soil classes, the SHPs of *Meyer et al.* [1997] and *Rawls et al.* [1982] yield similar soil moisture contents and more or less fall within the range of predicted SHPs-B. These findings put the physical meaning of SHPs into perspective and tend to characterize the SHPs as fitting parameters rather than as physical parameters. Nevertheless, large differences among the parameter prediction methods remain, especially for soils with high sand content.

[37] To assess whether the CP is also a good representation of the average temporal behavior in soil moisture, a window within the time series of θ_{daily} for the CP of the soil class ClL (chosen because of its central position on the texture triangle) is shown in Figure 11, together with the corresponding ensemble mean. It can be seen that the application of the CP in the SHPs agrees well with the ensemble mean and is able to capture all fluctuations in the mean soil-moisture content. Note that not all soil classes show the

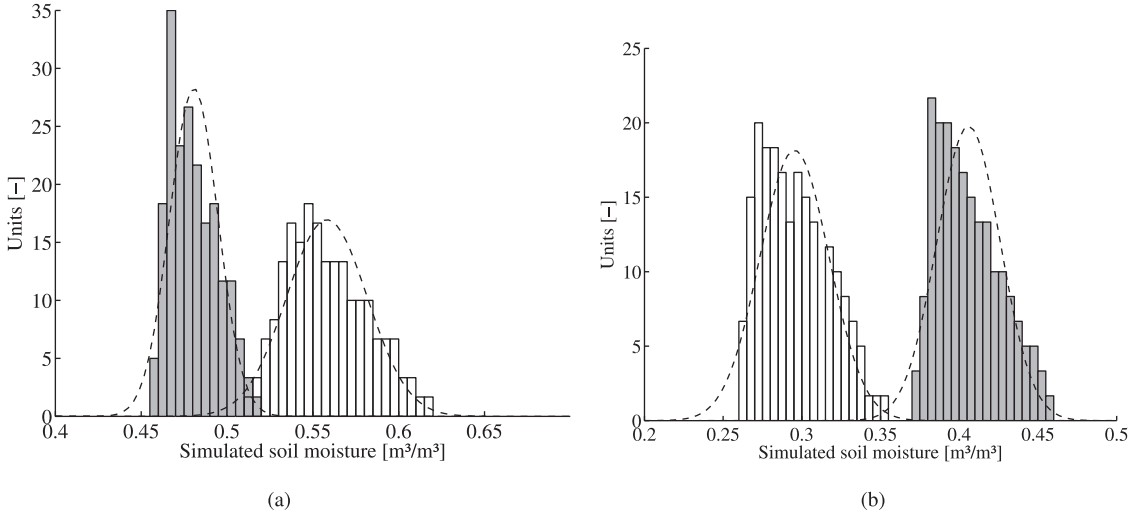

Figure 9. Probability distribution of the 2006 simulated soil-moisture content, θ_{daily}, using the SHPs predicted from PTF A (gray) and PTF B (white), in a silty clay soil on (a) a wet day (DOY 215) and (b) on a dry day (DOY 260). The full black line shows the corresponding normal distribution.

same perfect pattern, though the match between the CP and the mean appears to be very good. Irrespective of the PTF used, the CP seems to represent the average behavior in simulated soil moisture within a given soil class. The time series of θ_{daily} obtained with the SHPs from *Meyer et al.* [1997] and *Rawls et al.* [1982] are quite different from those obtained with the CP. The former show more or less the same behavior in θ_{daily} as in SHPs-A, but are shifted toward lower soil-moisture values (Figure 11). Despite the similar mean θ_{avg}, the literature-based SHPs are unable to generate a similar evolution in θ_{daily} as that obtained with SHPs-B. The former result in a more gradual wetting and drying of the soil with less extremes in the high and low soil-moisture values. These findings underline the need for a reliable estimation of SHPs in hydrologic modeling since SHPs have significant impact on modeled soil moisture and standard values for the SHPs may be inappropriate.

5. Conclusions

[38] The incorporation of uncertainty in model parameters is important for correct representations of the hydrologic model response. Unfortunately, modeling of uncertainty is not a standard practice in hydrologic modeling and there is a lack of framework for assessing parameter uncertainty and propagating the uncertainty through the model.

[39] In this paper, we dealt with two uncertainty issues related to simulations in basins where soil information is limited to a soil type map: (1) within-soil-class variability of SHPs, and (2) reliability of the PTF (region specific versus nonregion specific) used to estimate the SHPs. A methodology was presented to quantify the uncertainty in SHPs arising from the textural variability within soil classes and to propagate SHP distribution through a hydrologic model with conservation of its higher-order moments. The intention of the proposed method was not to provide the true SHP uncertainty, but to give a reliable estimate of uncertainty based on the application of continuous region-specific PTFs. The method was illustrated by means of a synthetic experiment. We have shown that the resulting SHP PDFs were nonnormally distributed, irrespective of the PTF used. However, a nonregion-specific PTF resulted in substantially different SHP uncertainty in comparison with a region-specific PTF, in terms of (1) the absolute SHP values, (2) the range in predicted SHPs, and (3) the shape of the distribution. These differences could be attributed to, among other factors, different numbers of samples in the data set, the geographic origin of the soil data (determining the climatic and soil conditions), and the methods used to measure the SHPs. Selecting the PTF is therefore a crucial step when assessing the uncertainty in SHPs. If region-specific PTFs are available, they are preferable over standard (often nonregion-specific) PTFs. In any case, PTFs remain poor predictors as long as the structure of the soil is not incorporated in the regression.

[40] The SHP PDFs were applied in a hydrologic model and were found to result in nonnormal distributions of the simulated soil-moisture content. Especially under very dry conditions, this nonnormality was found to be significant. A representative characterization of the uncertainty, hence, requires that higher-order moments of the distribution are taken into account. With respect to the application of data assimilation algorithms this implies that nonlinear filters should be used to account for nonnormal error distributions since neglecting the higher-order moments of the state's PDF may compromise assimilation results. In general, a substantial impact of the within-soil-class variability of SHPs on modeled soil moisture was observed. However, there were large differences between the region- and nonregion-specific PTFs with respect to the modeled soil-moisture uncertainty. These differences could be linked to the shape and spread of the SMRC and HCC. The consistent underestimation of soil moisture obtained with nonregion-specific PTFs as compared to region-specific PTFs suggested a fundamental deficiency in the regression equation in accounting for differences between soils from different geographic origins. It could therefore be argued that the choice of PTF is a crucial step when assessing the uncertainty in soil moisture since differences between PTFs remain after propagating their SHPs through a hydrologic

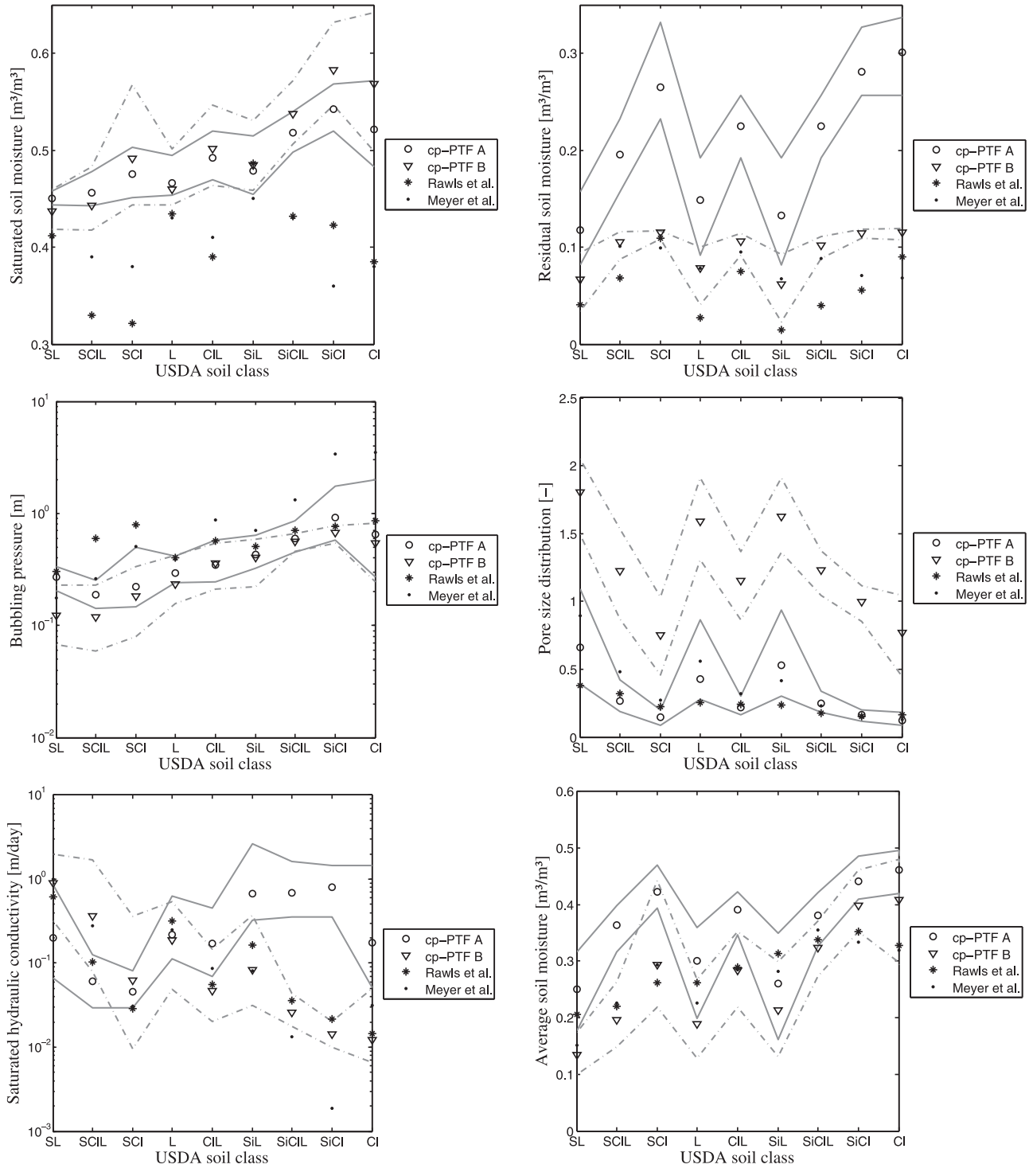

Figure 10. Range of the SHPs and θ_{avg} within each USDA soil class as predicted from PTF A (solid line) and PTF B (dotted line) with indication of the SHP for the central point (CP). Results are compared to standard SHPs reported by *Rawls et al.* [1982] and *Meyer et al.* [1997].

model. Furthermore, an accurate computation of the PDF (including elements of nonlinearity and nonnormality) is important if the uncertainty in soil-moisture content needs to be modeled accurately.

[41] In an analogy to common practice, a best guess SHP set was generated to obtain a quick assessment of the mean system behavior, using soil type information. Therefore, the CP, which corresponds to the center of gravity of a soil class, was selected as a representative texture sample for a given soil class. The SHPs of the CP were corresponded well with the mean SHPs of the soil class. Furthermore, the CP was found to represent the average behavior in modeled

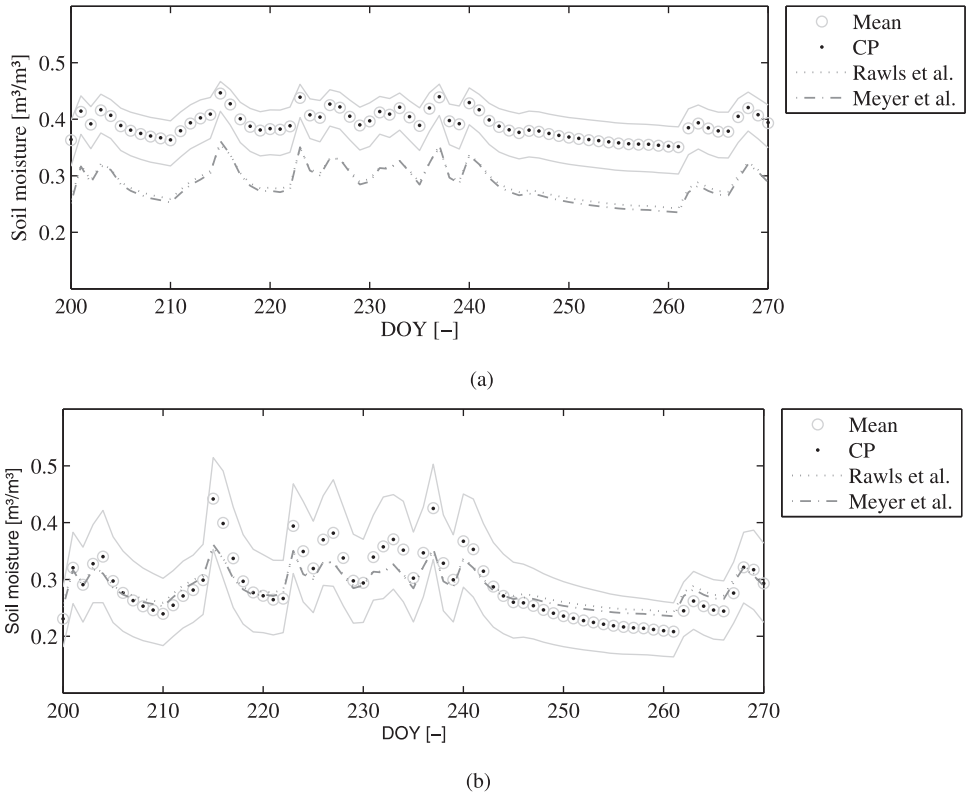

Figure 11. Time series of the ensemble mean of the simulated soil-moisture content, θ_{daily} resulting from (a) PTF A and (b) PTF B for the soil class clay loam with indication of the range in model output for comparison with the model run for the central point and with the SHPs taken from the work of *Rawls et al.* [1982] and *Meyer et al.* [1997].

soil-moisture content. Values for SHPs reported by *Rawls et al.* [1982] and *Meyer et al.* [1997] could not capture either the average soil moisture or the fluctuation in soil-moisture behavior obtained with the best guess SHPs. From these findings, we conclude that the CP is a useful tool to generate a more reliable behavior of mean soil moisture as compared to the standard class PTFs, since the CP allows for the use of continuous PTFs. In literature, there is a wider choice of the latter, and such PTFs are often available for a specific region of interest.

[42] In the future, more attention should be paid to appropriately addressing SHP uncertainty as a result of within-soil-class variability, since this generates a substantial amount of uncertainty in modeled soil moisture. Research should aim to develop methods that allow for fast and accurate assessment of uncertainty since current methods are time consuming and, hence, not feasible in practice. However, to obtain reliable estimates of uncertainty on the hydrologic model output, a reliable PTF needs to be selected and the PDF output need to be fully characterized (including the higher-order moments). When used in a data assimilation framework, it would be useful to assess the impact of the higher-order moments on assimilation results.

[43] **Acknowledgments.** This research was performed in the framework of project G.0837.10 funded by the Research Foundation Flanders (FWO). The authors would like to thank the Flemish Environment Agency (VMM) for providing meteorological and soil-moisture data. Gabriëlle De Lannoy is funded by a postdoctoral research grant from the FWO.

References

Benke, K. K., K. E. Lowell, and A. J. Hamilton (2008), Parameter uncertainty, sensitivity analysis and prediction error in a water-balance hydrological model, *Math. Comput. Modell.*, *47*(11–12), 1134–1149.

Bormann, H. (2008), Sensitivity of a soil-vegetation-atmosphere-transfer scheme to input data resolution and data classification, *J. Hydrol.*, *351*(1–2), 154–169.

Bouma, J. (1989), Using soil survey data for quantitative land evaluation, *Adv. Soil Sci.*, *9*, 177–213.

Brooks, R. H., and A. T. Corey (1964), Hydraulic properties of porous media, Hydrol. Pap. 3, 27 pp., Colo. State Univ., Fort Collins.

Cornelis, W. M., J. Ronsyn, M. Van Meirvenne, and R. Hartmann (2001), Evaluation of pedotransfer functions for predicting the soil moisture retention curve, *Soil Sci. Soc. Am. J.*, *65*(3), 638–648.

Cosby, B. J., G. M. Hornberger, R. B. Clapp, and T. R. Ginn (1984), A statistical exploration of the relationships of soil moisture characteristics to the physical properties of soils, *Water Resour. Res.*, *20*(6), 682–690, doi:10.1029/WR020i006p00682.

Famiglietti, J. S., and E. F. Wood (1994), Multiscale modeling of spatially variable water and energy balance processes, *Water Resour. Res.*, *30*(11), 3061–3078, doi:10.1029/94WR01498.

Finke, P. A., J. H. M. Wösten, and M. J. W. Jansen (1996), Effects of uncertainty in major input variables on simulated functional soil behaviour, *Hydrol. Processes*, *10*(5), 661–669.

Grayson, R. B., I. D. Moore, and T. A. McMahon (1992), Physically based hydrologic modeling, 2. Is the concept realistic?, *Water Resour. Res.*, *28*(10), 2659–2666, doi:10.1029/92WR01259.

Gutmann, E. D., and E. E. Small (2005), The effect of soil hydraulic properties vs. soil texture in land surface models, *Geophys. Res. Lett.*, *32*(2), L02402, doi:10.1029/2004GL021843.

Hopmans, J. W., J. Simunek, N. Romano, and W. Durner (2002), Simultaneous determination of water transmission and retention properties. inverse methods., in *Methods of Soil Analysis*, *Soil Sci. Soc. Am. Book*

Ser., Vol. 5, edited by J. H. Dane and G. C. Topp, pp. 963–1008, Soil Sci. Soc. Am., Madison, Wis.

Kaiser, K., and G. Guggenberger (2003), Mineral surfaces and soil organic matter, *Eur. J. Soil Sci.*, *54*(2), 219–236.

Mayer, L. M., L. L. Schick, K. R. Hardy, R. Wagal, and J. McCarthy (2004), Organic matter in small mesopores in sediments and soils, *Geochim. Cosmochim. Acta*, *68*(19), 3863–3872.

McBratney, A. B., B. Minasny, S. R. Cattle, and R. W. Vervoort (2002), From pedotransfer functions to soil inference systems, *Geoderma*, *109*(1–2), 125–152.

Meyer, P., M. Rockhold, and G. Gee (1997), Uncertainty analysis of infiltration and subsurface flow and transport for sdmp sites, *Rep. NUREG/CR-6565*, U.S. Nucl. Regul. Comm, Rockville, Md.

Minasny, B., and A. B. McBratney (2002), Uncertainty analysis for pedotransfer functions, *Eur. J. Soil Sci.*, *53*(3), 417–429.

Nemes, A., D. J. Timlin, Y. A. Pachepsky, and W. J. Rawls (2009), Evaluation of the Rawls et al. (1982), pedotransfer functions for their applicability at the U.S. national ccale, *Soil Sci. Soc. Am. J.*, *73*(5), 1638–1645.

Pauwels, V.R.N., A. Balenzano, G. Satalino, H. Skriver, N.E.C. Verhoest, and F. Mattia (2009), Optimization of soil hydraulic model parameters using synthetic aperture radar data: An integrated multidisciplinary approach, *IEEE Trans. Geosci. Remote Sens.*, *47*(2), 455–467.

Peters-Lidard, C. D., M. S. Zion, and E. F. Wood (1997), A soil-vegetation-atmosphere transfer scheme for modeling spatially variable water and energy balance processes, *J. Geophys. Res.*, *102*(D4), 4303–4324, doi:10.1029/96JD02948.

Rawls, W. J., and D. L. Brakensiek (1985), Prediction of soil water properties for hydrologic modelling, in *Watershed Management in the Eighties*, edited by E. Jones and T. J. Ward, pp. 293–299, Am. Soc. Civ. Eng., Proc. Symp., 30 April–1 May, Denver, Colo., Am. Soc. Civ. Eng., New York, N.Y.

Rawls, W. J., and D. L. Brakensiek (1989), Estimation of soil water retention and hydraulic properties, in *Unsaturated flow in hydrologic modelling: Theory and practice*, edited by H. Morel-Seytoux, pp. 275–300, Kluwer Acad., Dordrecht.

Rawls, W. J., D. L. Brakensiek, and K. E. Saxton (1982), Estimation of soil water properties, *Trans. Am. Soc. Agric. Eng.*, *25*(5), 1316–1320.

Refsgaard, J. C., and B. Storm (1996), Construction, calibration and validation of hydrological models, in *Distributed Hydrological Modelling*, edited by M. A. Abott and J. C. Refsgaard, pp. 41–54, Kluwer, Dordrecht.

Samain, B., B. V. A. Ferket, W. Defloor, and V.R.N. Pauwels (2011), Estimation of catchment averaged sensible heat fluxes using a Large Aperture Scintillometer, *Water Resour. Res.*, doi:10.1029/2009WR009032, in press.

Saxton, K. E., and W. J. Rawls (2006), Soil water characteristics estimates by texture and organic matter for hydrologic solutions, *Soil Sci. Soc. Am. J.*, *70*(5), 1569–1578.

Schaap, M. G., F. L. Leij, and M. T. van Genuchten (1998), Neural network analysis for hierarchical prediction of soil hydraulic properties, *Soil Sci. Soc. Am. J.*, *62*(4), 847–855.

Sivapalan, M., K. Beven, and E. F. Wood (1987), On hydrologic similarity, 2. a scaled model for runoff prediction, *Water Resour. Res.*, *23*(12), 2266–2278.

Sleutel, S., S. De Neve, B. Singier, and G. Hofman (2006), Organic C levels in intensively managed arable soils – long-term regional trends and characterization of fractions, *Soil Use Manage.*, *22*(2), 188–196.

Soet, M., and J.N.M. Stricker (2003), Functional behaviour of pedotransfer functions in soil water flow simulation, *Hydrol. Processes*, *17*(8), 1659–1670.

Tietje, O., and V. Hennings (1996), Accuracy of the saturated hydraulic conductivity prediction by pedo-transfer functions compared to the variability within fao textural classes, *Geoderma*, *69*(1–2), 71–84.

Tietje, O., and M. Tapkenhinrichs (1993), Evaluation of pedo-transfer functions, *Soil Sci. Soc. Am. J.*, *57*(4), 1088–1095.

Twarakavi, N. K. C., J. Šimůnek, and M. G. Schaap (2009), Development of Pedotransfer Functions for Estimation of Soil Hydraulic Parameters using Support Vector Machines, *Soil Sci. Soc. Am. J.*, *73*(5), 1443–1452, doi:10.2136/sssaj2008.0021.

Twarakavi, N. K. C., J. Šimůnek, and M. G. Schaap (2010), Can texture-based classification optimally classify soils with respect to soil hydraulics?, *Water Resour. Res.*, *46*, W01501, doi:10.1029/2009WR007939.

Vachaud, G., and T. Chen (2002), Sensitivity of computed values of water balance and nitrate leaching to within soil class variability of transport parameters, *J. Hydrol.*, *264*(1–4), 87–100.

van Genuchten, M. (1980), A closed-form equation for predicting the hydraulic conductivity of unsaturated soils, *Soil Sci. Soc. Am. J.*, *44*(5).

Vereecken, H., J. Feyen, J. Maes, and P. Darius (1989), Estimating the soil moisture retention characteristics from texture, bulk density and carbon content, *Soil Sci.*, *148*(6), 389–403.

Vereecken, H., J. Maes, and J. Feyen (1990), Estimating unsaturated hydraulic conductivity from easily measured soil properties, *Soil Sci.*, *141*(1), 1–12.

Wagner, B., V. R. Tarnawski, V. Hennings, U. Muller, G. Wessolek, and R. Plagge (2001), Evaluation of pedo-tranfer functions for unsaturated soil hydraulic conductivity using an independent data set, *Geoderma*, *102*(3–4), 275–297.

Walker, W. E., P. Harremoës, J. Rotmans, J. P. van der Sluis, M. B. A. V. Asselt, P. Janssen, and M. P. K. V. Krauss (2003), Defining uncertainty: A conceptual basis for uncertainty management in model-based decision support, *Integr. Assess.*, *4*(1), 5–17.

Webb, T. H., and L. R. Lilburne (2005), Consequences of soil map unit uncertainty on environmental risk assessment, *Aust. J. Soil Res.*, *43*(2), 119–126.

Wösten, J. H. M., A. Lilly, A. Nemes, and C. Le Bas (1999), Development and use of a database of hydraulic properties of European soils, *Geoderma*, *90*(3–4), 169–185.

Wösten, J. H. M., Y. A. Pachepsky, and W. J. Rawls (2001), Pedotransfer functions: bridging the gap between available basic soil data and missing soil hydraulic characteristics, *J. Hydrol.*, *251*(3-4), 123-150.

W. M. Cornelis, Department of Soil Management, Ghent University, Coupure Links 653, B-9000 Ghent, Belgium.

G. J. M. De Lannoy, L. Loosvelt, V. R. N. Pauwels, and N. E. C. Verhoest, Laboratory of Hydrology and Water Management, Ghent University, Coupure Links 653, B-9000 Ghent, Belgium. (Lien.Loosvelt@ugent.be)